polymers

MDPI

Article

Preparation and Performance of Ultra-Fine Polypropylene Antibacterial Fibers via Melt Electrospinning

Qiu-Sheng Li †, Hong-Wei He *,†, Zuo-Ze Fan, Ren-Hai Zhao, Fu-Xing Chen, Rong Zhou * and Xin Ning *

Industrial Research Institute of Nonwovens & Technical Textiles, College of Textiles & Clothing, Qingdao University, Qingdao 266071, China; 2017021401@qdu.edu.cn (Q.-S.L.); 2017021409@qdu.edu.cn (Z.-Z.F.); chinesezrh@126.com (R.-H.Z.); fuxing1991@gmail.com (F.-X.C.)

* Correspondence: hhwpost@163.com (H.-W.H.); rzhouqdu@126.com (R.Z.); xning@qdu.edu.cn (X.N.)

† These two authors contributed equally to this work.

Received: 22 January 2020; Accepted: 3 March 2020; Published: 6 March 2020

Abstract: Polypropylene (PP) fibers are employed commonly as the raw material of technical textiles (nonwovens), and the research focuses on fine-denier fibers and their functionalities. In this work, antibacterial PP masterbatches with different dosage (1–5 wt.%) of nano-ZnO particles as the antibacterial agent were prepared via a twin-screw extruder. The as-prepared PP masterbatches were electrospun on a home-made electrospinning device to afford ultra-fine PP fibers. The morphologies of as-spun ultrathin PP fibers with 16 μm of average diameter were observed by SEM. The structure and element distribution were characterized by means of energy-dispersive spectroscopy (EDS) and Fourier-transfer infrared spectroscopy (FTIR), respectively. There was some zinc obviously distributed on the surface when a dosage of ZnO more than 1 wt.% was used, which contributed to the antibacterial activity. The crystallinity of PP fibers was not affected strongly by the dosage of ZnO based on the differential scanning calorimetry (DSC) heating curves, while thermal decomposition improved with the increase in ZnO content, and the mechanical strength decreased predictably with the increase in inorganic ZnO content.

Keywords: melt electrospinning; PP fibers; ZnO; antibacterial fibers

1. Introduction

Polypropylene (PP) is a colorless, odorless, non-toxic organic polymer with chemical resistance, electrical insulation, high-strength mechanical properties, and good wear-resistant processing performance. PP and its composites are applied in many fields such as the machinery, automobile, electronics, textile, packaging, agriculture, forestry, fishery, and food industries [1]. With particular regard to technical textiles, following the rapid development of the chemical, environmental protection, energy, and other emerging industries, the development trend of fine-denier PP fibers is being focused, as well as their functionality [2–5].

In the last few decades, the electrospinning (e-spinning) technique attracted more and more attention because it is a facile method of preparing ultra-fine and functional fibers [6–8]. Based on the properties of precursors, the e-spinning strategies can be divided into three types: solution, melt, and novel solventless e-spinning [9]. In the solution e-spinning processes, the polymer solution is used as the precursor. The jet drawn by electrostatic force leaves the Taylor cone and then solidifies quickly with solvent volatilization [10]. Because of the environment concerns of organic solvents and low efficiency, solution e-spinning cannot be easily applied widely and industrialized. Novel types of

solventless e-spinning were developed, in which some liquid materials sensitive to light [11], heat [12], or moisture [13] are used as precursors, while the jets are initiated easily under these corresponding conditions to solidify quickly into fibers. However, these methods need more complicated devices to provide steady initiating conditions. Melt e-spinning utilizes polymer melts as precursors, which is close to spunbond, a spinning process for technical textiles [14,15]. The fibers produced by melt e-spinning are much finer than those produced by spunbond. The e-spinning conditions and fibrous morphologies of various melt polymers were previously reviewed [16]. Nayak et al. explored the melt e-spinning conditions of PP [17] and Kadomae et al. explained the relationship between the tactility and diameter of electrospun (e-spun) fibers [18]. Cho et al. investigated the conditions for melt e-spinning of PP and solution e-spinning of PP with dissolution in decalin, with the best results obtained at temperatures higher than 130 °C, and they also compared the e-spun PP ultrathin fibers produced via two different e-spinning methods with average diameters of 9.6 μm and 0.8 μm achieved [19].

Nano-ZnO is a kind of stable inorganic oxide, belonging to the n-type semiconductor family [20]. The electrons on the valence band of ZnO can accept an energy transition from ultraviolet rays, which can provide broad-spectrum ultraviolet protection [21,22], as well as antibacterial properties [23,24], and this material was verified to be safe and effective in the evaluation of sunscreen [25]. With concerns about the safety of heavy metals, such as nano-silver or its ions, more and more researchers began studying the antibacterial properties of nano-ZnO applied as a non-leaching additive [26], such as in cellulose filled with nano-ZnO to prepare an antibacterial lyocell [27], PP or PE doped with nano-ZnO as an antibacterial food packaging film [28], and antibacterial PP nonwovens with the addition of ZnO nanorods [29].

Nano-ZnO powder as an antibacterial additive was applied in some e-spinning precursors of soluble polymers, such as polylactide (PLA) [30], polyurethane (PU) [31], polycaprolactone (PCL) [32], poly (3-hydroxybutyrate) [33], etc. There are scarce reports on melt e-spinning to fabricate antibacterial fibers by adding nano-ZnO. In this research, a blending composite of commercial nano-ZnO in a PP matrix was prepared using a twin-screw machine, and antibacterial masterbatches were produced. A series of ultra-fine PP fibers with different proportions of nano-ZnO were afforded by melt e-spinning, and the morphology, structure, and mechanical and thermal properties of the fibers were analyzed. The antibacterial effect was also evaluated. The obtained fibers have promising application in the field of hygienic textiles.

2. Materials and Methods

2.1. Materials

PP (ExxonMobil™ 3155E5) was obtained from Shandong SWT New Material Technology Co.,Ltd. (Yantai, China), with a melt flow index of 35 g/10 min, and nano-ZnO was purchased from Boyu High Technique New Material Technology Co., Ltd. (Beijing, China), with an average particle size of 30 nm.

2.2. Preparation of PP Antibacterial Masterbatches

The masterbatches were prepared using a twin-screw extruder with a main feeder and a side feeder (16 mm Benchtop Twin-Screw Extrusion Pelletizing Line, Labtech Engineering Co., Ltd., Samutprakarn, Thailand). The pristine PP was charged from the main feeder and nano-ZnO particles were charged from the side feeder, blended in a ratio of 8:2 to prepare the 20 wt.% high-proportion antibacterial masterbatch. The temperature of each heating zone of the twin-screw extruder was set based on Table 1. Then, this masterbatch containing 20% ZnO was diluted by pristine PP in the same twin-screw extruder, thus obtaining PP antibacterial masterbatches with ZnO content of 1 wt.%, 2 wt.%, 3 wt.%, 4 wt.%, and 5 wt.%. The appearances of pristine PP and ZnO, as well as PP with 1 wt.% ZnO, are shown in Figure S1 (Supplementary Materials).

Table 1. The temperatures of heating zones of twin-screw extruder.

Heating Zones	1	2	3	4	5	6	7	8	9	10
Temperature (°C)	170	180	190	200	200	210	210	210	210	210

2.3. Home-Made Melt E-Spinning Device

A melt e-spinning device was built, as illustrated in Figure 1, which consisted of a heater with a controller, a high-voltage power source (HVPS, Tianjin Dongwen high voltage power company, Tianjin, China), a syringe connected with a nozzle and a pipeline of inert CO_2 gas to prevent oxidation, and a roller receiver connected to a positive electrode.

The prepared PP masterbatches with ZnO content of 0 wt.%, 1 wt.%, 2 wt.%, 3 wt.%, 4 wt.% and 5 wt.% were put into the metal syringe in turn and heated to 210 °C for 20 min while ventilating CO_2 gas into the metal syringe. This was followed by turning on the receiving roller and HVPS, with the voltage set to 30 kV. The PP melt exited the nozzle, forming a Taylor cone in the high electrostatic field. Then, the melt jet exited the Taylor cone and solidified into a fiber deposited on the receiver. All PP masterbatches were e-spun to give fibers PP-0, PP-1, PP-2, PP-3, PP-4, and PP-5 with ZnO content of 0 wt.%, 1 wt.%, 2 wt.%, 3 wt.%, 4 wt.%, and 5 wt.%, respectively.

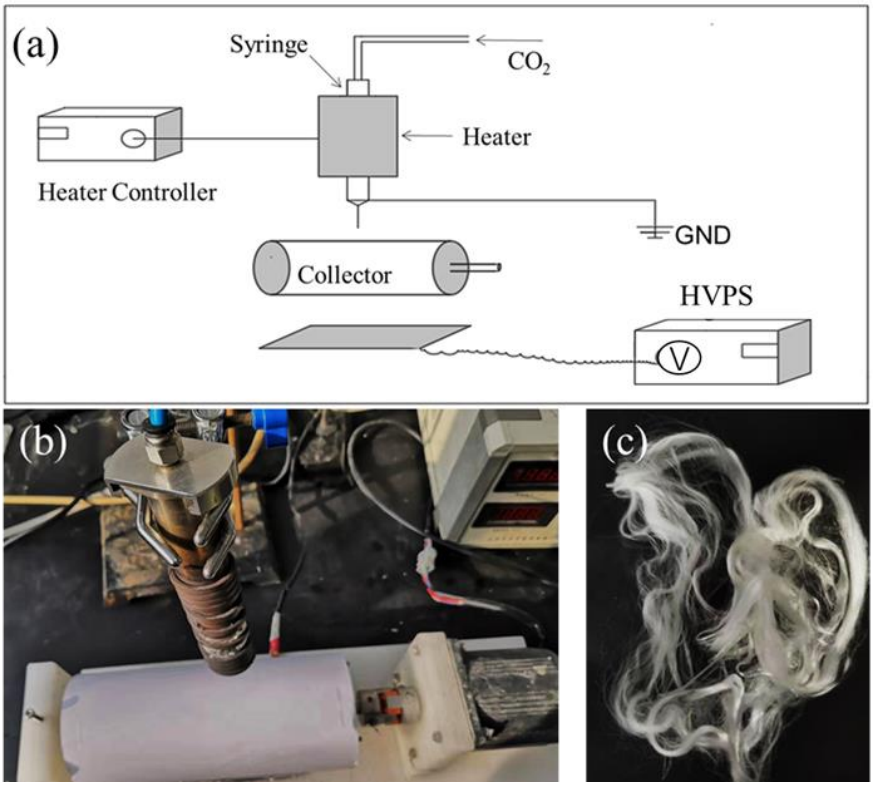

Figure 1. (**a**) Home-made melt e-spinning device; (**b**) heating device; (**c**) melt e-spun polypropylene (PP) fibers.

2.4. Characterization

The morphologies of e-spun fibers were observed by scanning electron microscopy (SEM, TESCAN-VEGA3, Kohoutovice, Czech). The structures and the elemental analysis of e-spun fibers were characterized by a Fourier-transform infrared spectroscope (FT-IR, Nicolet iS10, Thermo Fisher Scientific, Waltham, MA, USA) and an energy-dispersive spectrometer (EDS, SERIAL#: E1856-C2B, Brno, Czech), respectively. Furthermore, their strength was measured eight times for every sample on a FAVIMAT Fiber Test machine (FAVIMAT, TexTechno, Mönchengladbach, Germany), with a

tensile rate of 100 mm/min and a tensile length of 10 mm. The adopted stress–strain curve of every sample was close to the average values of all eight tests (see Figure S2, Supplementary Materials). The thermal properties of e-spun fiber were characterized by means of a thermogravimetry analyzer (TGA)/differential scanning calorimeter (DSC) 3 + (TA Q2000, TA Instruments, New Castle, DE, USA), in which the temperature of differential scanning calorimetry (DSC) was raised from 35 °C to 250 °C under an atmosphere of nitrogen. Every sample was tested three times on the DSC for averaging the thermal enthalpy. The thermogravimetric analyzer (TGA) was also implemented in an N_2 atmosphere. The temperature was raised from 35 °C to 700 °C, and the heating rate was 10 °C/min. The antibacterial property of the fibers was determined via an agar plate diffusion test based on the standard of GB/T 20944.1-2007 (China), and the inhibitory effects on *Escherichia coli* (E.C.) and *Staphylococcus aureus* (S.A.) were evaluated.

3. Results and Discussion

3.1. Morphologies of PPS E-Spun Fibers

As shown in Figures 2 and 3, the morphologies of e-spun PP fibers containing different contents of ZnO were observed by SEM. All e-spun fibers with or without ZnO were about 16 μm on average in diameter, which indicated that the e-spinning process and as-spun fibers were not affected strongly when adding inorganic nano-ZnO with content lower than 5 wt.%

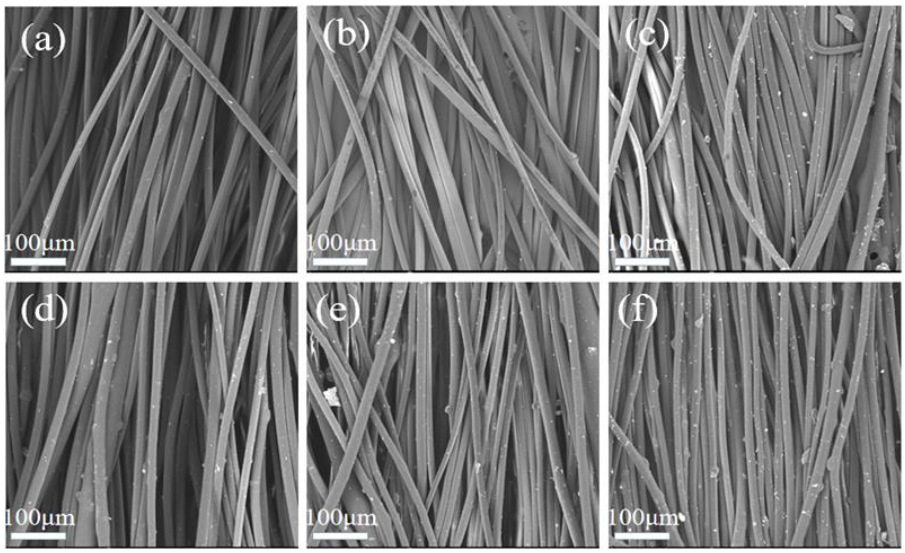

Figure 2. The SEM images of e-spun PP fibers containing ZnO: (**a**) 0 wt.%; (**b**) 1 wt.%; (**c**) 2 wt.%; (**d**) 3 wt.%; (**e**) 4 wt.%; (**f**) 5 wt.%.

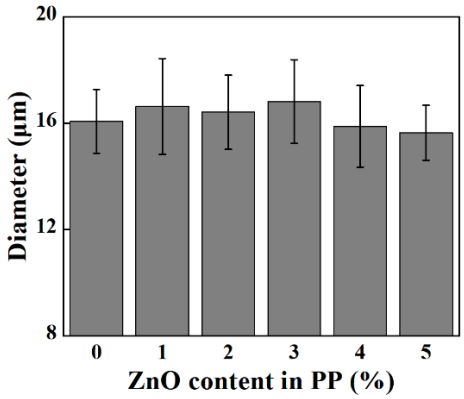

Figure 3. Average diameter of e-spun PP fibers.

SEM with energy-dispersive spectroscopy (SEM–EDS) was employed to show the element distribution on the surface of e-spun fibers. Although there were some ZnO particles embedded inside the e-spun PP fibers, others were distributed on the surface, as demonstrated by the EDS patterns (Figure 4). The content or density of zinc especially increased when the dosage increased. As shown in the FTIR spectra (Figure 5), the peaks at 2946 cm^{-1} and 2862 cm^{-1} were assigned to asymmetric and symmetric stretching vibrations of CH_3 of PP, and those at 2912 cm^{-1} and 2833 cm^{-1} were assigned to CH_2 of PP. The peak of 1459 cm^{-1} was attributed to the bending vibration of CH_2 of PP, and that at 1373 cm^{-1} was assigned to the deformation vibration of CH_3. The peak at 3435 cm^{-1} of ZnO may have originated from the stretching vibration of residual OH or moisture, as, after blending with PP in the extruder, it disappeared because of the high temperature or low dosage. All FTIR spectra of the e-spun PP fibers demonstrated that the PP structure, including crystalline type, was not changed [34].

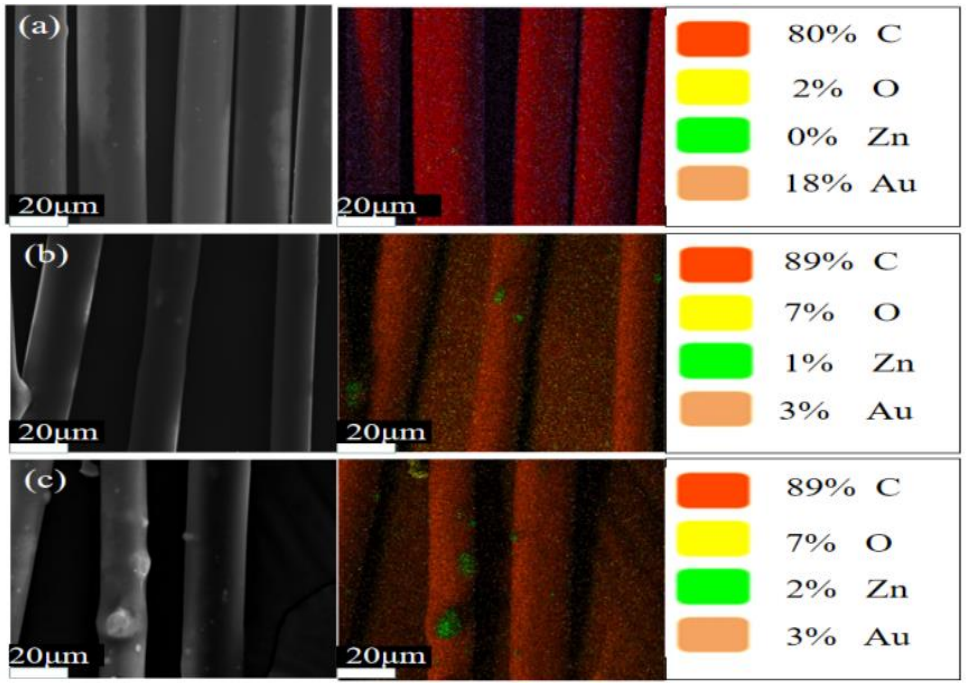

Figure 4. SEM/energy-dispersive spectroscopy (EDS) patterns of PP e-spun fibers containing ZnO: (**a**) 0 wt.%; (**b**) 1 wt.%; (**c**) 3 wt.%.

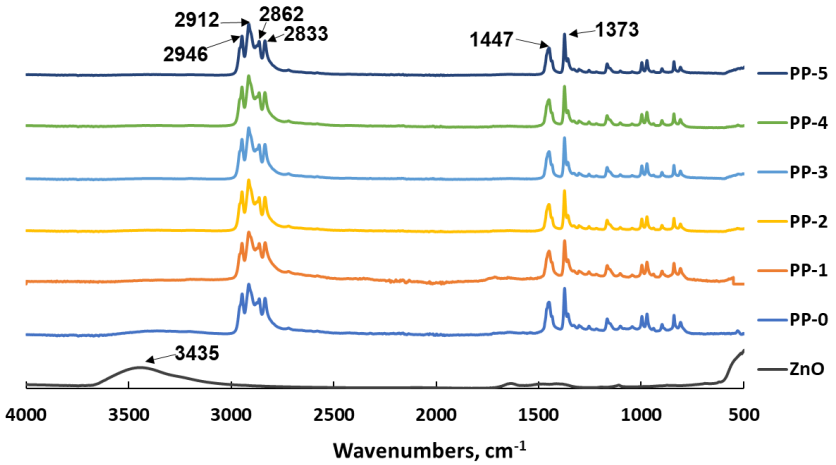

Figure 5. Fourier-transform infrared (FTIR) spectra of ZnO and e-spun PP fibers with different content of ZnO.

3.2. Thermal Properties of E-Spun PP Fiber

Figure 6a shows the DSC analysis of the fiber. The melting temperature of the PP fibers with different content of ZnO was between 168 and 170 °C, which shows that the addition of nano-ZnO particles did not affect the melting point of the PP fibers. The crystallinity of e-spun fibers was calculated as follows:

$$Xc = \Delta H_1/\Delta H_2, \quad (1)$$

where Xc is the crystallinity, ΔH_1 is the thermal enthalpy of the sample (J/g) given by measuring the peak area in the thermogram, and ΔH_2 is the thermal enthalpy of 100% crystalline PP (209 J/g) [35].

As shown in Figure 6b, the crystallinity of the e-spun fibers did not change greatly when the dosage of ZnO was lower than 4 wt.%. However, it decreased remarkably with the addition of ZnO higher than 5 wt.%, which indicated that more inorganic nanoparticles affected the crystallization.

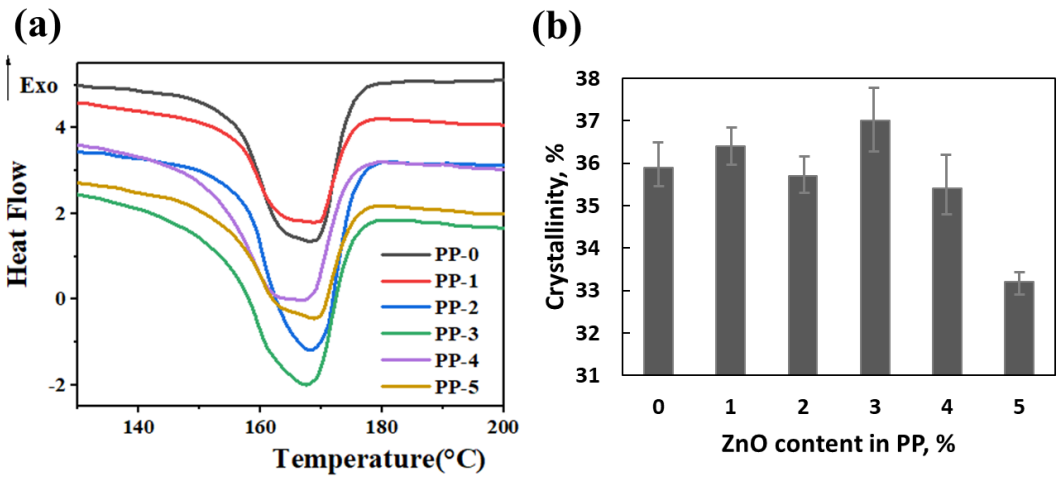

Figure 6. (**a**) Differential scanning calorimetry (DSC) heating curves and (**b**) crystallinities of PP fibers.

When ZnO nanoparticles were added to PP, the thermal decomposition temperature of the fibers increased. Based on the TG and DTG curves in Figure 7, the rate of fiber decomposition gradually increased with the increase in nano-ZnO content, and the thermal decomposition temperature constantly increased from 438 °C (PP-0) to 461 °C (PP-5). Because nano-ZnO has a large specific surface area, when it is dispersed in the PP matrix, it would inhibit the release of volatile thermal decomposition products, thus playing an important role in forming a barrier layer and further inhibiting the decomposition of the matrix [36].

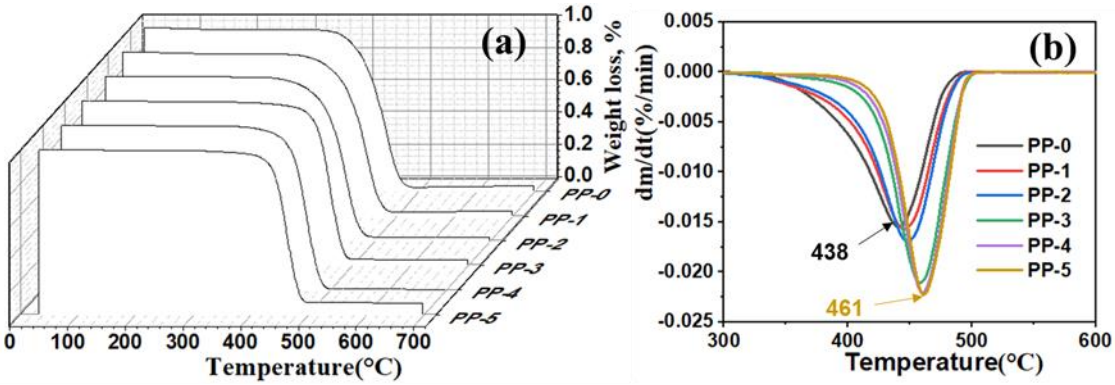

Figure 7. (**a**) Thermogravimetry (TG) traces of as-spun fibers and (**b**) differential TG (DTG) spectra.

3.3. Mechanical Tensile Properties of E-Spun PP Fibers

Due to their compatibility or dispersion with inorganic compounds, organic polymers, including PP, commonly suffer from a deterioration of mechanical performance when preparing composites or functional materials with inorganic materials. In this work, the introduction of nano-ZnO particles as an antibacterial additive also caused a reduction in the mechanical properties. The stress–strain behavior of the e-spun PP fibers was compared (Figure 8a), and the elongation at break and breaking strength were found to reduce with an increase in the content of ZnO (Figure 8b).

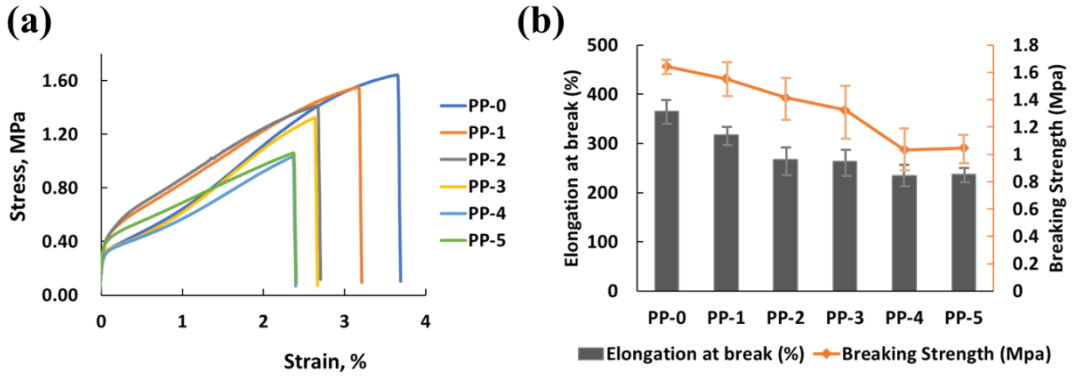

Figure 8. (**a**) Stress–strain behavior, and (**b**) trend of elongation at break and breaking strength of e-spun PP fibers.

3.4. Antibacterial Properties of E-Spun Fibers

The antibacterial mechanisms of ZnO were disclosed under different conditions. Under dark conditions, the antimicrobial activity of ZnO nanoparticles results from the attachment of ZnO to bacterial cell walls and a subsequent release of Zn^{2+} ions into the bacterial cytoplasm [37]. It is generally believed that the electrons (e^-) on the valence band of ZnO are excited and transition to the conduction band when they are irradiated by light with a photon energy larger than the band gap width, leaving a positively charged hole (h^+) on the valence band. The e− and h+ react with oxygen, hydroxyl, and water adsorbed on the surface of the substrate materials to form OH·, O_2^-, and H_2O_2. Among them, h^+ and OH· have very strong oxidation activity, which can break the chemical bond of most organic materials. Thus, they can decompose various components of microorganisms and be used to kill germs. In addition, O_2^- has a high reduction capacity and also plays a role in antibacterial performance [38–40].

$$ZnO + hv \rightarrow e^- + h^+ \quad (2)$$

$$h^+ + H_2O \rightarrow OH\cdot + H^+ \quad (3)$$

$$e^- + O_2 \rightarrow O_2^- \quad (4)$$

$$O_2^- + 2\,H^+ \rightarrow H_2O \quad (5)$$

The as-spun PP fibers were cut into pieces and put into agar solution (15 mL) which was added to the bacterial solution (the bacterial colony concentration was 1×10^8 colony-forming units (CFU)/mL), based on the national standard of agar plate diffusion (GB/T 20944.1-2007, China). After culturing for 24 h under a constant temperature of 36.5 °C, the inhibition effect of the fiber on *Escherichia coli* and *Staphylococcus aureus* was as shown in Figures 9 and 10. The pure PP fibers were used as control samples (Figures 9a and 10a). There were still many colonies, and there was no antibacterial ring, i.e., no antibacterial effect. The other PP fibers with different proportions of ZnO nanoparticles had obvious inhibition zones, i.e., an antibacterial effect, which was attributed to the nano ZnO particles migrating to the surface of the fibers.

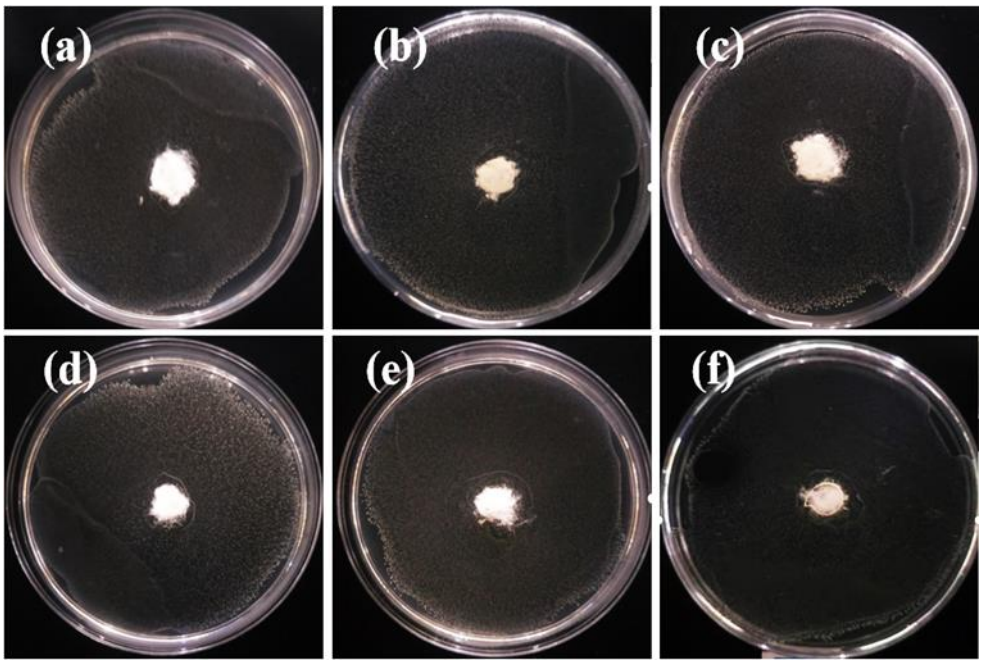

Figure 9. Antibacterial (*Escherichia coli*) activity measurements of e-spun PP fibers containing ZnO: (**a**) 0 wt.%; (**b**) 1 wt.%; (**c**) 2 wt.%; (**d**) 3 wt.%; (**e**) 4 wt.%; (**f**) 5 wt.%. The diameter of all containers was 9 cm.

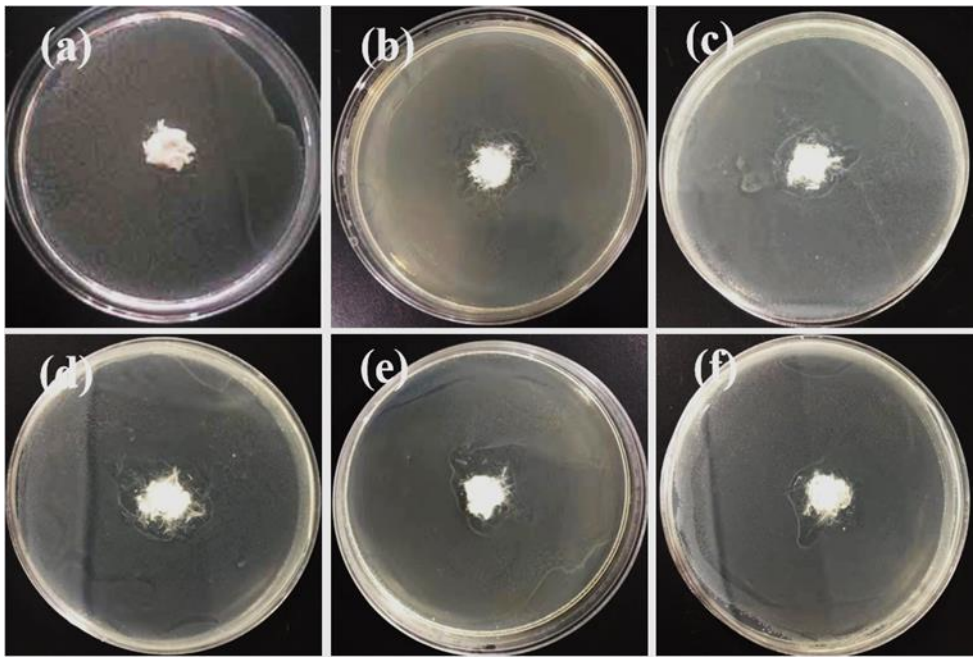

Figure 10. Antibacterial (*Staphylococcus aureus*) activity measurements of e-spun PP fibers containing ZnO: (**a**) 0 wt.%; (**b**) 1 wt.%; (**c**) 2 wt.%; (**d**) 3 wt.%; (**e**) 4 wt.%; (**f**) 5 wt.%. The diameter of all containers was 9 cm.

4. Conclusions

PP masterbatches containing different contents of nano-ZnO particles were prepared using a twin-screw extruder, and then applied as a melt e-spinning precursor to obtain ultra-fine fibers with antibacterial activity. The e-spun PP fibers were afforded with 16 μm of average diameter, and their structures and morphologies with or without nano ZnO were not changed remarkably. When ZnO

dosage was increased, the strength of the fibers decreased. Although the melting temperature and crystallinity of the e-spun fiber were not changed greatly, the thermal stability was effectively improved, as the decomposition temperature increased from 438 °C (PP-0) to 461 °C (PP-5). All e-spun PP fibers with ZnO dosages of 1 wt.%, 2 wt.%, 3 wt.%, 4 wt.%, and 5 wt.% were evaluated in terms of antibacterial performance, where even the 1 wt.% dosage of nano-ZnO particles could grant the e-spun PP fibers antibacterial activity against *Escherichia coli* and *Staphylococcus aureus*.

Supplementary Materials: The following are available online at http://www.mdpi.com/2073-4360/12/3/606/s1: Figure S1: The digital camera photo of pristine PP, nano-ZnO and PP blended with 1wt% ZnO; Figure S2: Stress-strain behaviors of e-spun PP fibers containing ZnO.

Author Contributions: Conceptualization, H.-W.H., R.Z., X.N., and R.-H.Z.; data curation, Q.-S.L.; formal analysis, Q.-S.L., H.-W.H., Z.-Z.F., and X.N.; methodology, Q.-S.L., H.-W.H., and X.N.; project administration, X.N.; validation, Q.-S.L., H.-W.H., R.Z., F.-X.C., and X.N.; writing—original draft preparation, Q.-S.L. and H.W.H.; writing—review and editing, Q.-S.L., H.-W.H., F.-X.C., R.Z., and X.N. All authors have read and agreed to the published version of the manuscript.

Funding: This research was supported by Major R&D Projects in Shandong Province (grant no.2019JZZY020220).

Conflicts of Interest: The authors declare no conflicts of interest.

References

1. Utracki, L.A.; Dumoulin, M.M. Polypropylene alloys and blends with thermoplastics. In *Polypropylene Structure, Blends and Composites*; Springer: Dordrecht, The Netherlands, 1995; pp. 50–94. [CrossRef]
2. Malkan, S.R. 9—Improving the use of polyolefins in nonwovens. In *Polyolefin Fibres*; Elsevier: Amsterdam, The Netherlands, 2017; pp. 285–311. [CrossRef]
3. Majchrzycka, K.; Okrasa, M.; Brochocka, A.; Urbaniak-Domagala, W. Influence of Low-Temperature Plasma Treatment on the Liquid Filtration Efficiency of Melt-Blown PP Nonwovens in the Conditions of Simulated Use of Respiratory Protective Equipment. *Chem. Process Eng.* **2017**, 195–207. [CrossRef]
4. Li, Y.; Chen, G.; He, J.; Han, Y.; Wang, X.; Kaplan, D. Silk-Based Biomaterials in Biomedical Textiles and Fiber-Based Implants. *Adv. Healthc. Mater.* **2015**, *4*. [CrossRef]
5. Peng, F.; Liu, D.; Zhao, W.; Zheng, G.; Ji, Y.; Dai, K.; Mi, L.; Zhang, D.; Liu, C.; Shen, C. Facile fabrication of triboelectric nanogenerator based on low-cost thermoplastic polymeric fabrics for large-area energy harvesting and self-powered sensing. *Nano Energy* **2019**, *65*, 104068. [CrossRef]
6. Mirjalili, M.; Zohoori, S. Review for application of electrospinning and electrospun nanofibers technology in textile industry. *J. Nanostruct. Chem.* **2016**, *6*. [CrossRef]
7. Cai, M.; He, H.; Zhang, X.; Yan, X.; Li, J.; Chen, F.; Yuan, D.; Ning, X. Efficient Synthesis of PVDF/PI Side-by-Side Bicomponent Nanofiber Membrane with Enhanced Mechanical Strength and Good Thermal Stability. *Nanomaterials* **2018**, *9*, 39. [CrossRef]
8. Dong, W.-H.; Liu, J.-X.; Mou, X.-J.; Liu, G.-S.; Huang, X.-W.; Yan, X.; Ning, X.; Russell, S.J.; Long, Y.-Z. Performance of polyvinyl pyrrolidone-isatis root antibacterial wound dressings produced in situ by handheld electrospinner. *Colloids Surf. B Biointerfaces* **2020**, *188*, 110766. [CrossRef]
9. Zhang, B.; Xu, Y.; He, H.-W.; Yu, M.; Ning, X.; Long, Y.-Z. Solvent-free Electrospinning: Opportunities and Challenges. *Polym. Chem.* **2016**, *8*. [CrossRef]
10. Lian, H.; Meng, Z. Melt electrospinning vs. solution electrospinning: A comparative study of drug-loaded poly (ε-caprolactone) fibres. *Mater. Sci. Eng. C* **2017**, *74*. [CrossRef] [PubMed]
11. He, H.-W.; Wang, L.; Xu, Y.; Zhang, L.-H.; Yu, M.; Yu, G.-f.; Dong, R.; Xia, L.; Ramakrishna, S.; Long, Y.-Z. Solvent-free electrospinning of UV curable polymer microfibers. *RSC Adv.* **2016**, *6*. [CrossRef]
12. Liu, S.-L.; Long, Y.-Z.; Huang, Y.-Y.; Zhang, H.-D.; He, H.-W.; Sun, B.; Sui, Y.-Q.; Xia, L.-H. Solventless electrospinning of ultrathin polycyanoacrylate fibers. *Polym. Chem.* **2013**, *4*. [CrossRef]
13. He, H.-W.; Zhang, B.; Xu, Y.; Dong, R.; Jia, X.; Yu, G.-f.; Ning, X.; Xia, L.; Long, Y.-Z. Solvent-free thermocuring electrospinning to fabricate ultrathin polyurethane fibers with high conductivity by in situ polymerization of polyaniline. *RSC Adv.* **2016**, *6*. [CrossRef]
14. Zhang, L.-H.; Duan, X.-P.; Xu, Y.; Yu, M.; Ning, X.; Zhao, Y.; Long, Y.-Z. Recent Advances in Melt Electrospinning. *RSC Adv.* **2016**, *6*. [CrossRef]

15. Fan, Z.-Z.; He, H.-W.; Yan, X.; Zhao, R.-H.; Long, Y.-Z.; Ning, X. Fabrication of Ultrafine PPS Fibers with High Strength and Tenacity via Melt Electrospinning. *Polymers* **2019**, *11*, 530. [CrossRef] [PubMed]
16. Hutmacher, D.; Dalton, P. Melt Electrospinning. *Chem. Asian J.* **2011**, *6*, 44–56. [CrossRef] [PubMed]
17. Nayak, R.; Padhye, R.; Kyratzis, I.; Truong, Y.; Arnold, L. Effect of viscosity and electrical conductivity on the morphology and fiber diameter in melt electrospinning of polypropylene. *Text. Res. J.* **2013**, *83*, 606–617. [CrossRef]
18. Kadomae, Y.; Maruyama, Y.; Sugimoto, M.; Taniguchi, T.; Koyama, K. Relation between tacticity and fiber diameter in melt-electrospinning of polypropylene. *Fibers Polym.* **2009**, *10*, 275–279. [CrossRef]
19. Cho, D.; Zhou, H.; Cho, Y.; Audus, D.; Joo, Y. Structural properties and superhydrophobicity of electrospun polypropylene fibers from solution and melt. *Poly* **2010**, *51*, 6005–6012. [CrossRef]
20. Shim, M.; Philippe, G.-S. Organic-Capped ZnO Nanocrystals: Synthesis and n-Type Character. *J. Am. Chem. Soc.* **2001**, *123*, 11651–11654. [CrossRef]
21. Becheri, A.; Dürr, M.; Lo Nostro, P.; Baglioni, P. Synthesis and characterization of zinc oxide nanoparticles: Application to textiles as UV-absorbers. *J. Nanopart. Res.* **2008**, *10*, 679–689. [CrossRef]
22. AbdElhady, M. Preparation and Characterization of Chitosan/Zinc Oxide Nanoparticles for Imparting Antimicrobial and UV Protection to Cotton Fabric. *Int. J. Carbohydr. Chem.* **2012**. [CrossRef]
23. Sharma, D.; Rajput, J.; Kaith, B.S.; Kaur, M.; Sharma, S. Synthsis of ZnO nanoparticals and study of their antibacterial and antifungal properties. *Thin Solid Films* **2010**, *519*, 1224–1229. [CrossRef]
24. Li, J.H.; Hong, R.; Li, M.; Li, H.Z.; Zheng, Y.; Ding, J. Effects of ZnO nanoparticles on the mechanical and antibacterial properties of polyurethane coatings. *Prog. Org. Coat.* **2009**, *64*, 504–509. [CrossRef]
25. Schilling, K.; Bradford, B.; Castelli, D.; Dufour, E.; Nash, J.; Pape, W.; Schulte, S.; Tooley, I.; Bosch, J.; Schellauf, F. Human Safety Review of "nano" Titanium Dioxide and Zinc Oxide. *Photochem. Photobiol. Sci.* **2010**, *9*, 495–509. [CrossRef] [PubMed]
26. Kuo, J.; Fan, C.-C.; Su, T.-L.; Chen, S.-H.; Lan, W. Nano composite fiber process optimization for polypropylene with antibacterial and far-infrared ray emission properties. *Text. Res. J.* **2016**, *86*. [CrossRef]
27. Malis, D.; Jeršek, B.; Tomšič, B.; Štular, D.; Golja, B.; Kapun, G.; Simončič, B. Antibacterial Activity and Biodegradation of Cellulose Fiber Blends with Incorporated ZnO. *Materials* **2019**, *12*, 3399. [CrossRef]
28. Espitia, P.J.P.; Soares, N.d.F.F.; Coimbra, J.S.d.R.; de Andrade, N.J.; Cruz, R.S.; Medeiros, E.A.A. Zinc Oxide Nanoparticles: Synthesis, Antimicrobial Activity and Food Packaging Applications. *Food Bioprocess Technol.* **2012**, *5*, 1447–1464. [CrossRef]
29. Fakoori, E.; Karami, H. Preparation and characterization of ZnO-PP nanocomposite fibers and non-woven fabrics. *J. Text. Inst.* **2018**, *109*, 1–7. [CrossRef]
30. Rodríguez-Tobías, H.; Morales, G.; Ledezma, A.; Romero, J.; Grande, D. Novel antibacterial electrospun mats based on poly(D,L-lactide) nanofibers and zinc oxide nanoparticles. *J. Mater. Sci.* **2014**, *49*. [CrossRef]
31. Tijing, L.; Ruelo, M.; Amarjargal, A.; Pant, H.; Park, C.-H.; Kim, D.; Kim, C. Antibacterial and superhydrophilic electrospun polyurethane nanocomposite fibers containing tourmaline nanoparticles. *Chem. Eng. J.* **2012**, *197*, 41–48. [CrossRef]
32. Augustine, R.; Malik, H.; Kumar, D.; Mukherjee, A.; Malakar, D.; Kalarikkal, N.; Thomas, S. Electrospun polycaprolactone/ZnO nanocomposite membranes as biomaterials with antibacterial and cell adhesion properties. *J. Polym. Res.* **2014**, *21*. [CrossRef]
33. Rodríguez-Tobías, H.; Morales, G.; Grande, D. Electrospinning and Electrospraying Techniques for Designing Antimicrobial Polymeric Biocomposite Mats. *Nanofiber. Res.* **2016**, *5*, 91–106.
34. Nakaoki, T.; Yamanaka, T.; Ohira, Y.; Horii, F. Dynamic FT-IR Analysis of the Crystallization to the Planar Zigzag Form for Syndiotactic Polypropylene. *Macromolecules* **2000**, *33*. [CrossRef]
35. Awad, A.; Elgamsy, R.; El-Wahab, A.; Hazem Abdellatif, M. Mechanical behavior of PP reinforced with marble dust. *Constr. Build. Mater.* **2019**, *228*, 116766. [CrossRef]
36. Bai, J.; Liao, X.; Huang, E.; Luo, Y.; Yang, Q.; Li, G. Control of the cell structure of microcellular silicone rubber/nanographite foam for enhanced mechanical performance. *Mater. Des.* **2017**, *133*, 288–298. [CrossRef]
37. Joe, A.; Park, S.H.; Shim, K.D.; Kim, D.J.; Jhee, K.H.; Lee, H.W.; Heo, C.H.; Kim, H.M.; Jang, E.S. Antibacterial mechanism of ZnO nanoparticles under dark conditions. *J. Ind. Eng. Chem.* **2017**, *45*, 430–439. [CrossRef]
38. Shi, L.E.; Li, Z.H.; Zheng, W.; Zhao, Y.F.; Jin, Y.F.; Tang, Z.X. Synthesis, antibacterial activity, antibacterial mechanism and food applications of ZnO nanoparticles: A review. *Food Addit. Contam. Part A* **2014**, *31*, 173–186. [CrossRef]

39. Ong, C.B.; Ng, L.Y.; Mohammad, A.W. A review of ZnO nanoparticles as solar photocatalysts: Synthesis, mechanisms and applications. *Renew. Sustain. Energy Rev.* **2018**, *81*, 536–551. [CrossRef]
40. Ton, N.Q.T.; Le, T.N.T.; Kim, S.; Dao, V.A.; Yi, J.; Vu, T.H.T. High-Efficiency Photo-Generated Charges of ZnO/TiO2 Heterojunction Thin Films for Photocatalytic and Antibacterial Performance. *J. Nanosci. Nanotechnol.* **2020**, *20*, 2214–2222. [CrossRef]